

Effects of Die Geometry on Cell Nucleation of PS Foams Blown With CO₂

XIANG XU, CHUL B. PARK*, DONGLAI XU, and REMON POP-ILIEV

*Microcellular Plastics Manufacturing Laboratory
Department of Mechanical and Industrial Engineering
University of Toronto
5 King's College Road
Toronto, Ontario, Canada M5S 3G8*

This paper investigates the effect of varying the geometry of the die on the cell nucleation behavior of extruded PS foams blown with CO₂. Three interchangeable groups of carefully calibrated filamentary dies have been used in the experimental study. The dies were deliberately designed to have either different pressure drop rates while having identical die pressures and flow rates, or different die pressures while having identical pressure drop rates and flow rates. The experimental results revealed that the geometry of the die governs the cell density of extruded PS foams, especially because of its significant effect on the pressure drop rate across the die. However, the effect of the die back pressure on the cell density was found to be marginal, whereas its effect on the cell morphology was found to be predominant. In addition, regardless of die geometry, the CO₂ content proved to be a very sensitive parameter with respect to the cell nucleation behavior of extruded PS foams. On the other hand, the cell density was slightly improved by an increase of the talc content, especially at reduced concentrations of CO₂.

INTRODUCTION

Foamed polymer products possess many unique characteristics compared to their solid counterparts, such as higher specific tensile strength, higher toughness, and better thermal and sound insulation properties. Generally, in plastic foams, the cell density, volume expansion ratio, and cell size determine the internal structure, and hence the final properties of foams. However, only two of these parameters are independent. For example, for a fixed expansion ratio, the cell size becomes smaller as the cell density increases. Since plastic foams having a smaller cell size and a more uniform cell size distribution exhibit better properties (1–8), substantial research efforts have been made to decrease the cell size by increasing the cell density. In this context, the cell-nucleating behaviors during foaming have been studied extensively for the purpose of increasing the cell density, especially for microcellular plastics processing (9–22).

Microcellular plastics are characterized by cell sizes less than 10 μm, and cell densities higher than 10⁹ cells/cm³. The initial concept for microcellular plastics

was conceived in response to an industrial need for reducing the material cost for certain polymer products without compromising the mechanical properties (23). Typically, microcellular plastics exhibit higher impact strength, higher toughness, higher stiffness-to-weight ratio, longer fatigue life, higher thermal stability, lower dielectric constant, lower thermal conductivity, and better light reflectability (1–8). In recent years, as a result of intensive research and development and because of their unique characteristics, these products have been commercialized and applied in broader fields (24–26).

BACKGROUND

The first-generation continuous-microcellular extrusion based process was developed by Park *et al.* (9–12). In this process, a polymer is melted in an extrusion barrel, and a metered amount of gas is delivered to the polymer melt stream under a high pressure. The injected gas diffuses into the polymer matrix at a fast rate because of the convective diffusion caused by the high shear rate in the extrusion barrel and the increased diffusivity at an elevated temperature. This leads to the formation of a single-phase polymer/gas solution (9, 10). The polymer/gas solution is then subjected to a thermodynamic instability to

*Corresponding author, park@mie.utoronto.ca.

This paper was presented at "Emerging Technologies for the New Millennium," held in Montreal, Dec. 10–11, 2001.

nucleate microcells. This is usually achieved by rapidly dropping the solubility of gas in the polymer melt by controlling the temperature and/or pressure at the nucleation die (9–11). Briefly, three major steps have been involved in producing microcellular foams: 1) polymer/gas solution formation, 2) cell nucleation, 3) cell growth, stabilization, and shaping. The cell nucleation process can occur homogeneously throughout the material or heterogeneously at high energy regions such as phase boundaries (27–31). In an ideal case, nucleation could occur instantaneously. The cell growth process is controlled primarily by the time allowed for the cells to grow, the temperature of the system, the state of supersaturation, the hydrostatic pressure or stress applied to the polymer matrix, and the viscoelastic properties of the polymer/gas solution (32). The final foam structure is determined by the conditions under which the three steps of the process are performed.

Formation of a homogeneous solution from the two-phase polymer/gas mixture is essential in continuous microcellular foam processing (10), because both the number and uniformity of bubbles nucleated are strongly dependent on the quality of the solution. Therefore, it must be first ensured that a correct amount of blowing agent is injected into the barrel to mix with and dissolve into the polymer. Since excess gas will form large voids, it would be important to determine the amount of blowing agent that can be absorbed and dissolved into the polymer (i.e., the solubility limit) at processing conditions. For the PS/CO₂ system, the solubility of CO₂ is estimated to be 9 wt% for 27.6 MPa (4000 psi) at 200°C (33).

The nucleation of numerous cells is critically important in microcellular processing because a microcellular structure would not be formed otherwise. Typically, a thermodynamic instability induced by a rapid drop in the gas solubility has been utilized in extrusion microcellular processing (9–11). Recently, there have been some efforts to utilize a shear strain to further increase the cell density by decreasing the activation energy for cell nucleation in a continuous microcellular processing (15, 17). It has been reported that a high shear could create a large cell density because of the high shear energy generated (30, 31). The influence of nucleating agent on cell nucleation was also investigated (14, 16, 29, 34). It has been observed that adding the nucleating agent is a favorable factor for cell nucleation even in the CO₂-based processing and that the effectiveness of the nucleating agent depends on the type and amount of blowing agent and on the polymer matrix.

In a previous study (10), Park *et al.* demonstrated the effect of the pressure-drop rate on cell nucleation in foam processing of HIPS with CO₂ while using three dies that had the same die pressure but different pressure-drop rates. They verified that the pressure-drop rate has a significant effect on cell nucleation through the induced thermodynamic instability. Different pressure-drop rates would induce different levels

of thermodynamic instability, and thereby different cell densities. The highest thermodynamic instability would occur when the pressure dropped most rapidly, which was exactly when the highest cell density was obtained. However, this study failed to show the comprehensive strategies on die design because the diameter and length of the dies were varied in such a way that the pressure was maintained to be constant while the pressure-drop rate was changed. Furthermore, experiments were conducted only at a fixed content of the blowing agent (i.e., CO₂), and consequently, the effect of CO₂ content on cell nucleation at various pressures and pressure-drop rates was not studied. Also, no nucleating agent was used, and therefore, the sensitivity of the cell density to the content of the nucleating agent at various die parameters was not investigated in the said study.

In order to study the effects of these well-known material and die-geometry parameters on the cell-nucleating behavior of extruded foams, a systematic research has been conducted by employing a set of dies with differing geometry in a foaming extruder while separately varying the contents of nucleating agent and blowing agent. For a given die geometry, the die pressure and pressure-drop rate are uniquely determined at each flow rate of polymer melt. Conversely, a unique die geometry can be determined for each set of the die pressure and pressure-drop rate at a given flow rate. With this rationale, three distinct groups of filamentary dies were designed and implemented in this study to investigate the effects of the die geometry on cell nucleation. Although a simple straight-filamentary die is chosen in this study, the developed concept can be extended to the design of converging-filamentary dies, straight-sheet dies, and converging-sheet dies.

DESIGN OF DIES

Assuming that the viscosity of the polymer/gas solution is shear-rate dependent and could be described by the "power law" in the flow through a tube (35, 36), the pressure drop, Δp , over the length of a nozzle for a non-Newtonian fluid in a fully developed flow can be expressed as (37):

$$-\Delta p = 2m \frac{L}{R^{3n+1}} \left[\left(3 + \frac{1}{n} \right) \frac{Q}{\pi} \right]^n \quad (1)$$

In order to derive the pressure-drop rate of the die, the residence time should be determined. The average residence time, Δt , of the flowing polymer/gas solution in the nozzle can be expressed as:

$$\Delta t \approx \frac{L}{v_{avg}} = \frac{L}{Q/\pi R^2} = \frac{\pi R^2 L}{Q} \quad (2)$$

Therefore, the pressure-drop rate can be estimated as follows:

$$\frac{dp}{dt} \approx \frac{\Delta p}{\Delta t} = -2m \left(3 + \frac{1}{n} \right)^n \left(\frac{Q}{\pi R^3} \right)^{n+1} \quad (3)$$

Equations 1 and 3 can be rewritten to express the pressure and the pressure-drop rate as a function of the die-geometry parameters and the melt flow rate.

$$\Delta p = A \cdot Q^n \cdot \left(\frac{L}{R^{3n+1}} \right) \quad (4)$$

$$\frac{\Delta p}{\Delta t} = B \cdot Q^{n+1} \cdot \frac{1}{R^{3n+3}} \quad (5)$$

where A and B are constants determined by the power-law characteristics of polymer melt:

$$A = -\frac{2m}{\pi^n} \cdot \left(3 + \frac{1}{n} \right)^n \quad (6)$$

$$B = -\frac{2m}{\pi^{n+1}} \cdot \left(3 + \frac{1}{n} \right)^n \quad (7)$$

From Eq 4, it is noted that in order to keep the same pressure drop at the same flow rate, the die lengths should be varied according to the different die diameters. More interestingly, Eq 5 shows that in a filament flow case, the pressure-drop rate is the function of only Q and R provided that m and n values are constant over the shear-rate range of the flow. This illustrates that for the same melt flow, as long as the die diameter is kept the same, the pressure-drop rate would be constant in spite of different pressure drops and die lengths. Therefore, if we fix the melt flow rate and change the die diameter, different levels of pressure-drop rates can be specifically achieved.

Equations 4 and 5 can be rewritten for R and L as a function of Δp , $\frac{\Delta p}{\Delta t}$, and Q :

$$R = B^{\frac{1}{3n+3}} \cdot Q^{\frac{1}{3}} \cdot \left(\frac{\Delta p}{\Delta t} \right)^{-\frac{1}{3n+3}} \quad (8)$$

$$L = A^{-1} \cdot B^{\frac{3n+1}{3n+3}} \cdot Q^{\frac{1}{3}} \cdot \Delta p \cdot \left(\frac{\Delta p}{\Delta t} \right)^{-\frac{3n+1}{3n+3}} \quad (9)$$

Equations 8 and 9 show that for a desired set of the pressure and the pressure-drop rate, the die parameters are uniquely determined at a given flow rate. Based

on this rationale, three groups of dies, 9 in total and 3 in each group, were designed in this study such that each die has a different pressure drop and different pressure-drop rate. The die diameter was kept unchanged within each die group, and thereby the pressure-drop rate was kept constant, while the die length was varied to produce three different levels of die pressures.

This study specifically considers foaming of polystyrene as a case example. The characteristic constants of PS, $m = 15,490 \text{ N}\cdot\text{s}^{0.333}/\text{m}^2$ and $n = 0.333$, which were determined from the rheological data within the shear rate ranging between 10^1 and 10^4 s^{-1} at 210°C , were used in the calculation.

The detailed design procedure is described as follows. First, the volumetric flow rate was set to $1.68\text{E}-7 \text{ m}^3/\text{s}$, which is a typical value for the specific extrusion system used in this study. Second, three levels of pressure drops of 13.8 MPa (2000 psi), 20.7 MPa (3000 psi), and 27.6 MPa (4000 psi), were selected. Then, three levels of pressure-drop rates of 0.082 GPa/s, 0.416 GPa/s, and 4.16 GPa/s were also selected. Within the same die group, the die diameters (i.e., the pressure-drop rates) were kept the same while the die lengths were varied to produce the aforementioned 3 levels of pressure drop. For different die groups, the die diameter was varied to have different pressure-drop rates. The geometric dimensions of the three groups of designed dies are summarized in Table 1. The relevant information about pressure drop and pressure-drop rate for each die could be observed in Fig. 1. Considering the three designed die groups, as shown in Fig. 1, Dies 1, 2, and 3, i.e., the dies in Group 1, have the same slope in the plot of pressure vs. time, meaning that they have the same pressure-drop rate (4.16 GPa/s); on the other hand, the die pressure drop occurs at three different levels (13.8 MPa, 20.7 MPa, and 27.6 MPa) as the die length is varied. Similarly, Dies 3, 4, and 5 in Group 2 and Dies 6, 7, and 8 in Group 3 have the same pressure-drop rates within each group at three die pressure levels. It should also be noted that Dies 1, 4, and 7 have the same die pressure level (27.6 MPa), Dies 2, 5, and 8 have the same die pressure level (20.7 MPa), and

Table 1. Calculated Geometry, Residence Time, and Pressure Drop Rate of the Dies for PS Having a Pressure Drop of 27.6 MPa, 20.7 MPa, and 13.8 MPa, Respectively.

Die Group	Die No.	Required Pressure Drop, MPa (psi)	Die Diameter, mm (inches)	Die Length, mm (inches)	Average Residence Time, s	Pressure Drop Rate, GPa/s
Group 1	Die 1	27.6 Mpa (4000 psi)	0.4572 mm (0.018 in)	6.79 mm (0.27 in)	0.0033	4.160
	Die 2	20.7 Mpa (3000 psi)	0.4572 mm (0.018 in)	5.09 mm (0.20 in)	0.0050	4.160
	Die 3	13.8 Mpa (2000 psi)	0.4572 mm (0.018 in)	3.39 mm (0.13 in)	0.0066	4.160
Group 2	Die 4	27.6 Mpa (4000 psi)	0.8128 mm (0.032 in)	21.46 mm (0.84 in)	0.0331	0.416
	Die 5	20.7 Mpa (3000 psi)	0.8128 mm (0.032 in)	16.10 mm (0.63 in)	0.0497	0.416
	Die 6	13.8 Mpa (2000 psi)	0.8128 mm (0.032 in)	10.73 mm (0.42 in)	0.0663	0.416
Group 3	Die 7	27.6 Mpa (4000 psi)	1.2192 mm (0.048 in)	48.29 mm (1.90 in)	0.1677	0.082
	Die 8	20.7 Mpa (3000 psi)	1.2192 mm (0.048 in)	36.22 mm (1.43 in)	0.2516	0.082
	Die 9	13.8 Mpa (2000 psi)	1.2192 mm (0.048 in)	24.15 mm (0.95 in)	0.3354	0.082

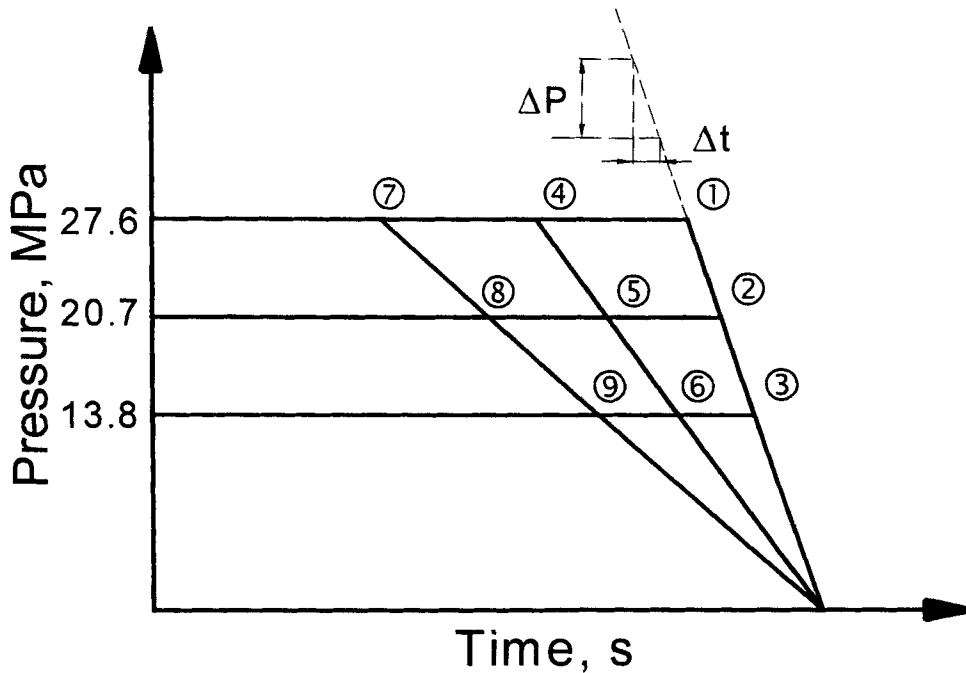


Fig. 1. Design of a series of 9 dies and the comparison of the pressure drop rate pertaining to different dies.

Dies 3, 6, and 9 have the same die pressure level (13.8 MPa). Using this combination of die designs, the effects of die geometry on cell nucleation can be systematically investigated.

CHARACTERIZATION OF FOAMS

The cell density, N_0 , is defined as the number of cells per cubic centimeter relative to the non-foamed material, and it is calculated by Eq 10 and 11 (6):

$$V_f = 1 - \frac{\rho_f}{\rho} \quad (10)$$

$$N_0 = \left(\frac{NM^2}{\alpha} \right)^{3/2} \left[\frac{1}{1 - V_f} \right] \quad (11)$$

Since the cell density is a quantitative parameter that directly reflects cell nucleation, it will be considered as the principal parameter to describe the nucleating behaviors of extruded PS foam in this study.

There are two different ways of counting the cell density: The first is to count the number of cells per unit volume with respect to foamed polymer, and the second is with respect to non-foamed polymer. Both are useful for different purposes. The first way is traditional and easier to understand and to characterize the foam itself in real life (38). In fact, most scholars working in the structure or property characterization field want to use the cell density with respect to the foamed volume because this is a more realistic and easier parameter to describe the structure and property. But the second way is defined to better describe the processing-to-structure relationships. Since the

foam processing consists of cell nucleation and cell growth, there has been a strong desire to describe the final cell morphology in terms of cell nucleation and growth behaviors. In other words, by defining the cell density as the cell-nuclei density (without any consideration of the expansion in this stage), the cell density can be used to indicate how well cell nucleation was conducted. So to speak, the cell density is meant to be the cell-nuclei density indicating the number of cells nucleated in the polymer matrix in the stage of cell nucleation. Since this is a paper on plastic foaming, the cell density calculated with respect to the non-foamed polymer was used to characterize the foam structure.

EXPERIMENTAL

Materials

The plastic material used in this study was PS 101 from Nova Chemicals. The MFI of this material is 2.2 g/10 min. The blowing agent used in the experiments was CO₂ (Matheson, 99.5%). Talc was used as a nucleating agent. The talc size ranged from 3 to 5 μm.

Experimental Setup

A schematic of the experimental extrusion setup used in this study is shown in Fig. 2. The setup consists of a 7.5 hp variable speed drive (Brabender Plasticorder EPL-V7752), a 3/4" extruder (Brabender 05-25-000) with a mixing screw of 30:1 L/D ratio (Brabender, 05-00-144) for plasticating the polymer pellets and dispersing the injected blowing gas throughout the melt, a positive displacement pump

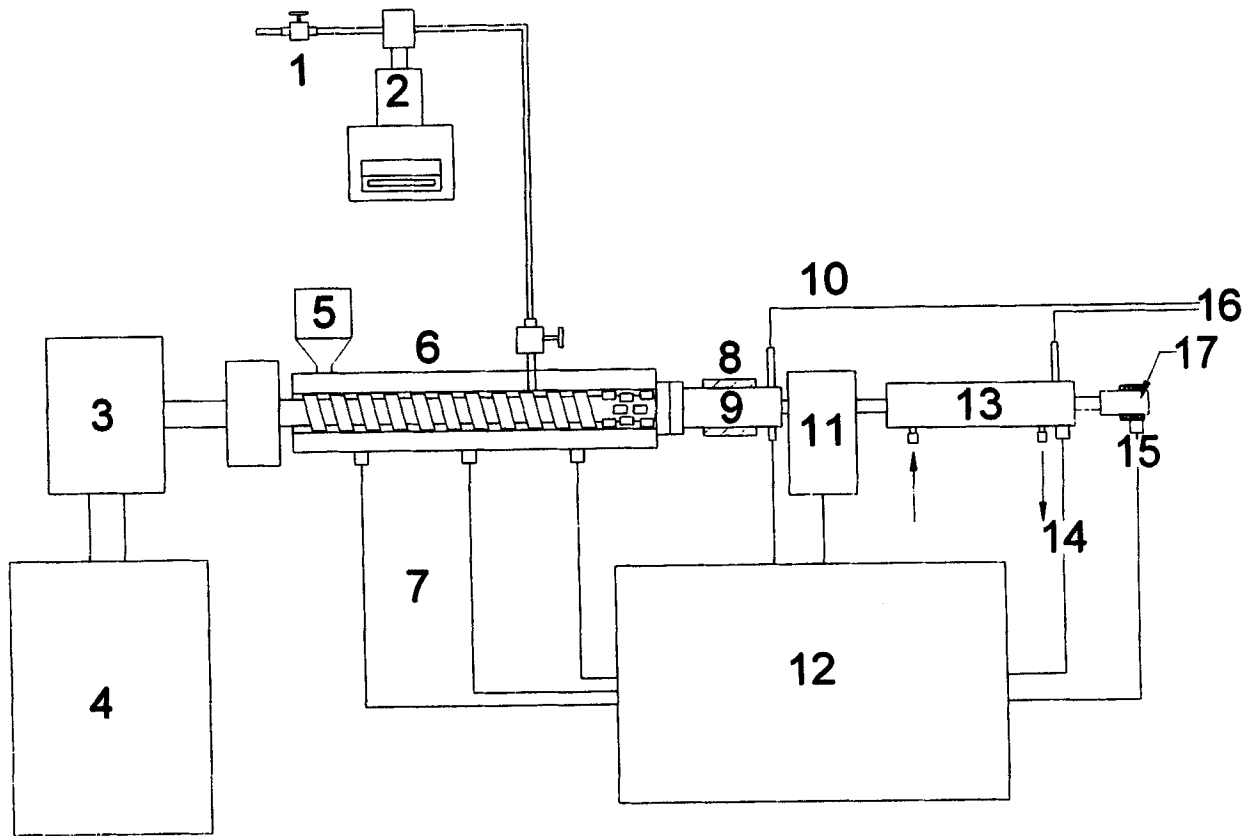


Fig. 2. Schematic of the experimental system setup. (1) blowing agent supply valve; (2) positive displacement pump; (3) gear box; (4) variable speed DC motor; (5) hopper; (6) extruder; (7) thermocouples; (8) heater; (9) mixing device; (10) pressure transducers; (11) gear pump; (12) control panel; (13) heat exchanger; (14) melt temperature; (15) nozzle temperature; (16) to control panel; (17) nucleation die.

for injecting the blowing gas, a six-element static mixer of diameter 6.8 mm (Omega FMX-84441-S) for enhancing the polymer/gas solution formation, a gear pump (Zenith, PEP-II 1.2 cc/rev) for controlling the melt flow rate, a heat exchanger containing homogenizing static mixers (Labcore, Model H-04669-12) for homogenizing the melt temperature, a gas injection port for injecting the blowing gas, six band heaters, four pressure transducers (Dynisco PT462B-10M-6/18) for detecting the pressures at various important locations, and six temperature controllers and six thermocouples for controlling the temperatures of the extrusion barrel, the mixer, the heat exchanger, the gear pump, and the die.

Calibration of the Dies

Since the actual relationship between the flow rate and the pressure drop in a die would be different from the theoretically predicted one most likely because of the ignored entrance pressure drop and the undeveloped flow in the entrance region, it was necessary to conduct a calibration experiment for each die to obtain the desired flow conditions (11). In the calibrations, Die 1 with the diameter of 0.457 mm (0.018") and the length of 6.79 mm (0.270") in the first group was selected as the reference. With this die mounted,

the polymer flow rate was measured to be $2.35\text{E-}7$ m^3/s , 1.4 folds the predicted value, when the die pressure was adjusted to 27.6 MPa (4000 psi) at 210°C. This actual value was used in all the calibrations of other dies.

First, calibration was conducted on Dies 4 and 7 so that they can have the same flow rate and die pressure as Die 1. The lengths of Dies 4 and 7 were originally made very long but cut in stages until the die pressures read 27.6 MPa (4000 psi) at the fixed flow rate of $2.35\text{E-}7$ m^3/s . Then using these 3 dies, calibration was conducted for all the other dies within each die group. In Group 1, the lengths of Dies 2 and 3 were cut in stages until the die pressures read the desired values of 13.8 MPa and 20.7 MPa, respectively at the fixed flow rate of $2.35\text{E-}7$ m^3/s . Similarly, calibration of die Group 2 (Dies 4–6) and Group 3 (Dies 7–9) was also conducted. Table 2 summarizes the calibrated die geometry.

The calibration of 9 dies at a fixed temperature (210°C), at a fixed die pressure (27.6 MPa), and at a fixed gas content (0%) is justified based on the assumption that the power-law index (n) would be maintained as the temperature, pressure, and gas content are varied. In other words, once dies are calibrated to have the same resistance at a temperature,

Table 2. Calibrated Geometry of the Dies for PS Having a Pressure Drop of 27.6 MPa, 20.7 MPa, and 13.8 MPa, Respectively.

Die Group	Die No.	Die Diameter, mm (inches)	Die Length, mm (inches)
Group 1	Die 1	0.4572 mm (0.018 in)	6.79 mm (0.27 in)
	Die 2	0.4572 mm (0.018 in)	5.59 mm (0.22 in)
	Die 3	0.4572 mm (0.018 in)	3.81 mm (0.15 in)
Group 2	Die 4	0.8128 mm (0.032 in)	35.56 mm (1.4 in)
	Die 5	0.8128 mm (0.032 in)	21.59 mm (0.85 in)
	Die 6	0.8128 mm (0.032 in)	14.22 mm (0.56 in)
Group 3	Die 7	1.2192 mm (0.048 in)	68.58 mm (2.7 in)
	Die 8	1.2192 mm (0.048 in)	50.80 mm (2.0 in)
	Die 9	1.2192 mm (0.048 in)	34.04 mm (1.34 in)

pressure, and gas content, then the resistance of the dies will be almost the same with respect to each other, although the temperature, pressure, and gas concentration changed as long as the power-law index is the same as shown below.

Consider Dies 1 and 4 at two different conditions "i" and "f". Equation 1 can be used to describe the pressure-drop rate and melt flow relationships for all these cases.

$$-\Delta p_{1i} = 2m_i \frac{L_1}{R_1^{3n_i+1}} \left(3 + \frac{1}{n_i}\right)^{n_i} \left(\frac{Q_{1i}}{\pi}\right)^{n_i} \quad (12)$$

$$-\Delta p_{4i} = 2m_i \frac{L_4}{R_4^{3n_i+1}} \left(3 + \frac{1}{n_i}\right)^{n_i} \left(\frac{Q_{4i}}{\pi}\right)^{n_i} \quad (13)$$

$$-\Delta p_{1f} = 2m_f \frac{L_1}{R_1^{3n_f+1}} \left(3 + \frac{1}{n_f}\right)^{n_f} \left(\frac{Q_{1f}}{\pi}\right)^{n_f} \quad (14)$$

$$-\Delta p_{4f} = 2m_f \frac{L_4}{R_4^{3n_f+1}} \left(3 + \frac{1}{n_f}\right)^{n_f} \left(\frac{Q_{4f}}{\pi}\right)^{n_f} \quad (15)$$

By dividing Eqs 12 and 14 using Eqs 13 and 15, respectively, one can have:

$$\frac{\Delta p_{1i}}{\Delta p_{4i}} = \left(\frac{Q_{1i}}{Q_{4i}}\right)^{n_i} \cdot \left(\frac{L_1}{R_1^{3n_i+1}}\right) \bigg/ \left(\frac{L_4}{R_4^{3n_i+1}}\right) \quad (16)$$

$$\frac{\Delta p_{1f}}{\Delta p_{4f}} = \left(\frac{Q_{1f}}{Q_{4f}}\right)^{n_f} \cdot \left(\frac{L_1}{R_1^{3n_f+1}}\right) \bigg/ \left(\frac{L_4}{R_4^{3n_f+1}}\right) \quad (17)$$

If the calibration is conducted at "i" condition to have the same Q and Δp for Dies 1 and 4, then Eq 16 becomes

$$\frac{L_1}{R_1^{3n_i+1}} = \frac{L_4}{R_4^{3n_i+1}} \quad (18)$$

and L_4 is calculated from this equation. With this L_4 value, Eq 17 becomes now,

$$\frac{\Delta p_{1f}}{\Delta p_{4f}} = \left(\frac{Q_{1f}}{Q_{4f}}\right)^{n_f} \cdot \left(\frac{R_1}{R_4}\right)^{3(n_i - n_f)} \quad (19)$$

In order for Δp_{1f} and Δp_{4f} to be the same for the same Q_{1f} and Q_{4f} , should be equal to n_i . Therefore, as long

as the power-law index remains the same, the calibration of dies will be effective even though the temperature, pressure, and/or gas content are changed.

It is known that the power-law index "n" for a given range of shear rate tends to increase as the viscosity drops by increasing the temperature, by decreasing the pressure, and/or by increasing the gas content (39). Since the actual foaming temperature range is below the calibration temperature and the actual gas content is higher than the calibration gas content, the power-law index in the actual foaming conditions is not expected to deviate much from that of calibration. It should also be noted that the entrance pressure drop (40), which has not been considered in this analysis, may cause some errors in the calibration, and a further study is required to clarify this issue.

Experimental Procedure

The PS resins were processed using the foaming experimental setup (Fig. 2), and a metered amount of CO₂ was injected into the PS melt. Using the 9 dies, experiments were carried out at various levels of CO₂ content, talc content, and die temperature.

The die temperature was carefully varied from 170°C to 120°C with a decrement of 5°C. The pressure changes with the decrease of temperature were recorded at the steady state of each processing condition. The CO₂ contents were 2 wt%, 5 wt%, and 10 wt%, and the talc contents were 0 wt%, 1 wt%, and 2 wt%. The foam samples were randomly selected at each processing condition and were characterized in terms of the cell density defined in Eqs 10 and 11.

RESULTS AND DISCUSSION

Extensive experiments were conducted by exposing each of the three specially designed groups of calibrated dies (shown in Table 2) to various processing conditions. The obtained experimental results were then plotted for various material and processing parameter combinations. For example, Fig. 3 shows the cell densities obtained at various temperatures using different dies with and 1% talc and 5% CO₂ contents. In order to clearly demonstrate the effects of the pressure-drop rate, die pressure, CO₂ content, and talc content on the cell density, the experimental results are plotted as a function of these parameters in Figs. 4–8

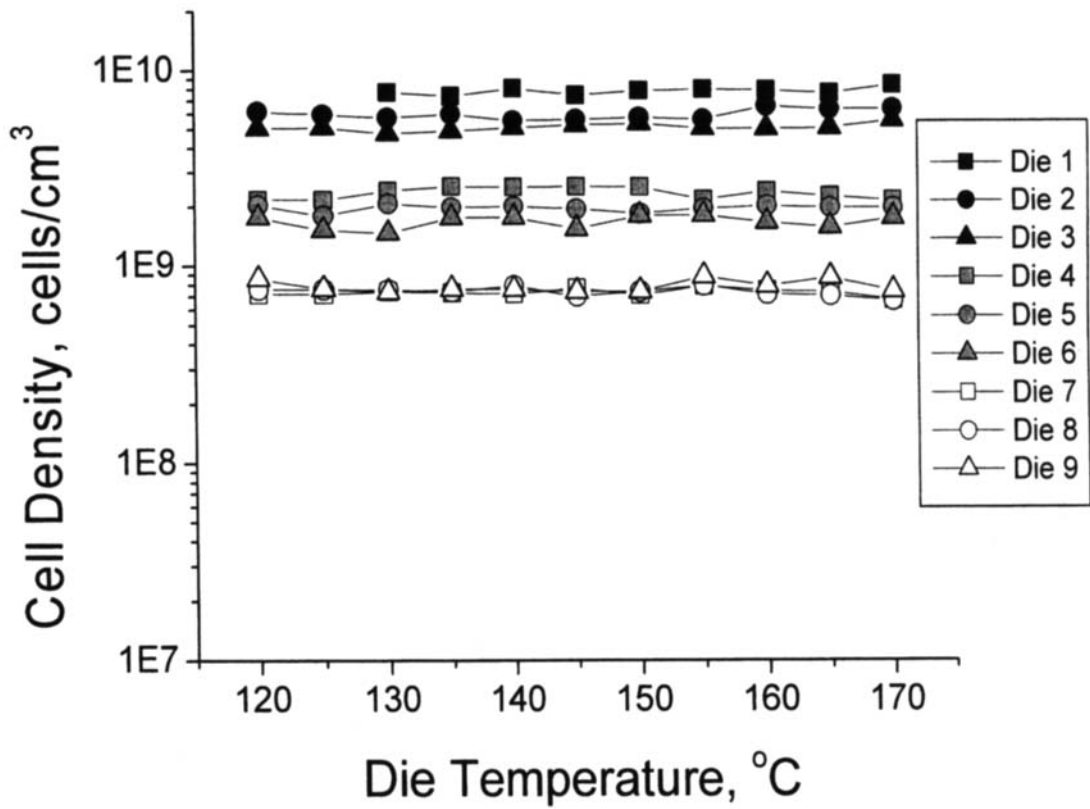


Fig. 3. Cell densities obtained at various die temperatures using a variety of dies with 1% talc and 5% CO₂ contents.

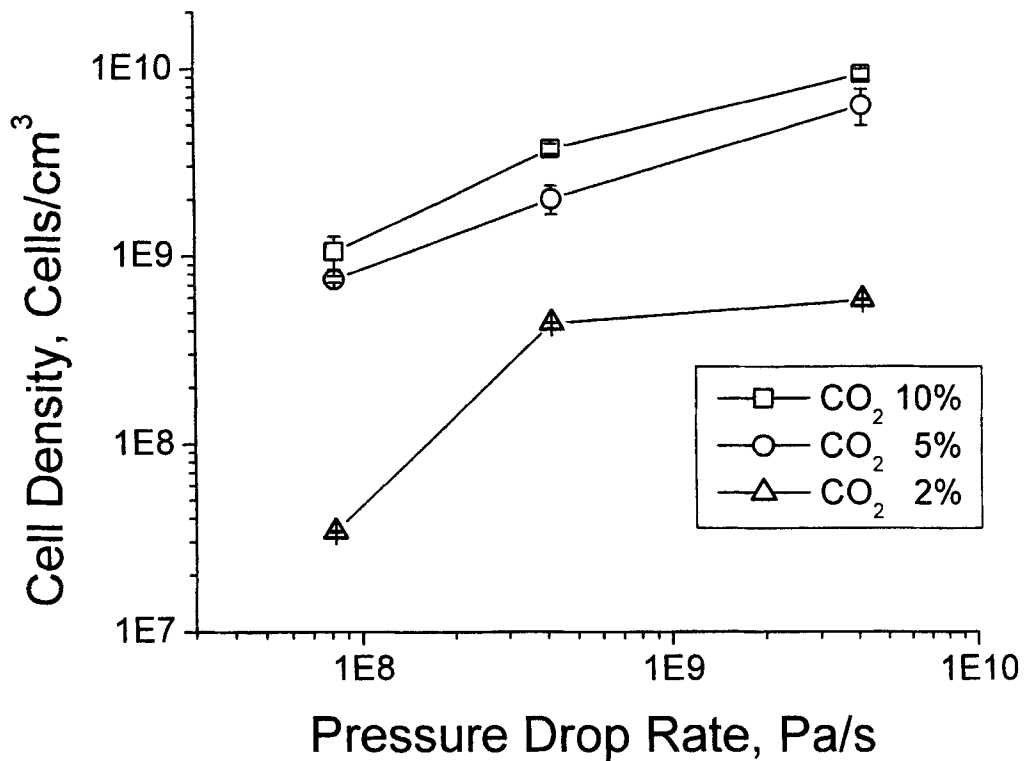


Fig. 4. Cell densities obtained at various die pressure drop rates with 1% talc.

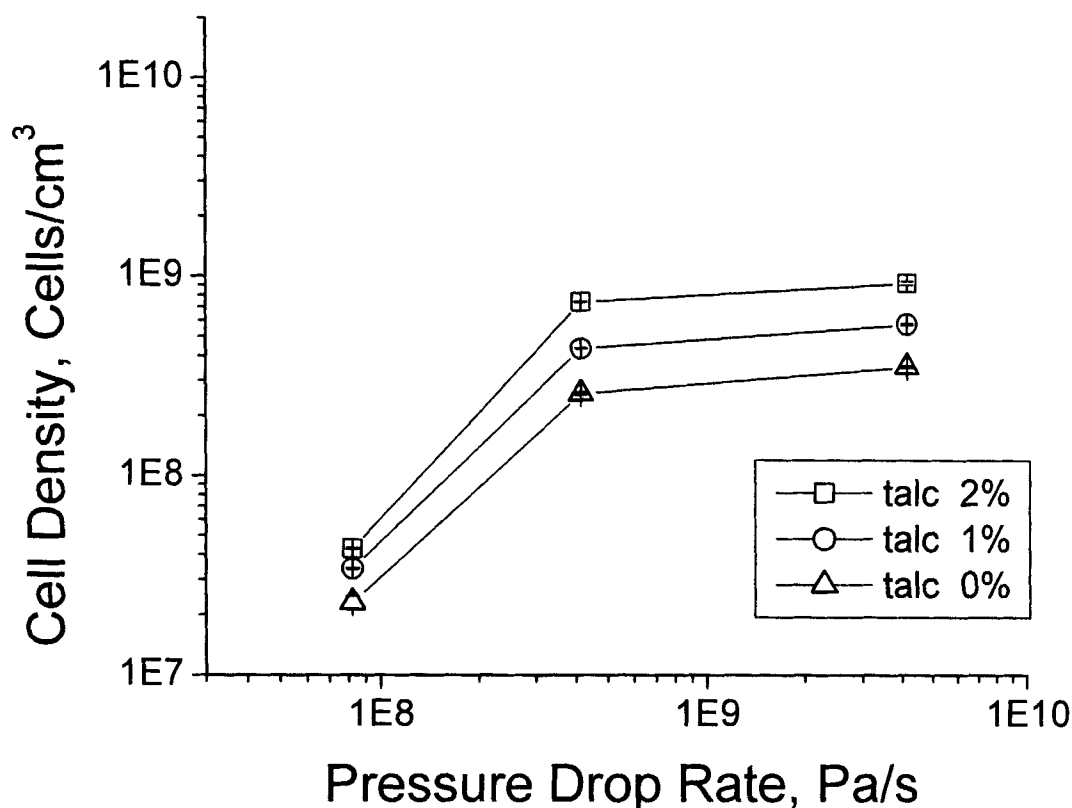


Fig. 5. Cell densities obtained at various die pressure drop rates with 2% CO₂.

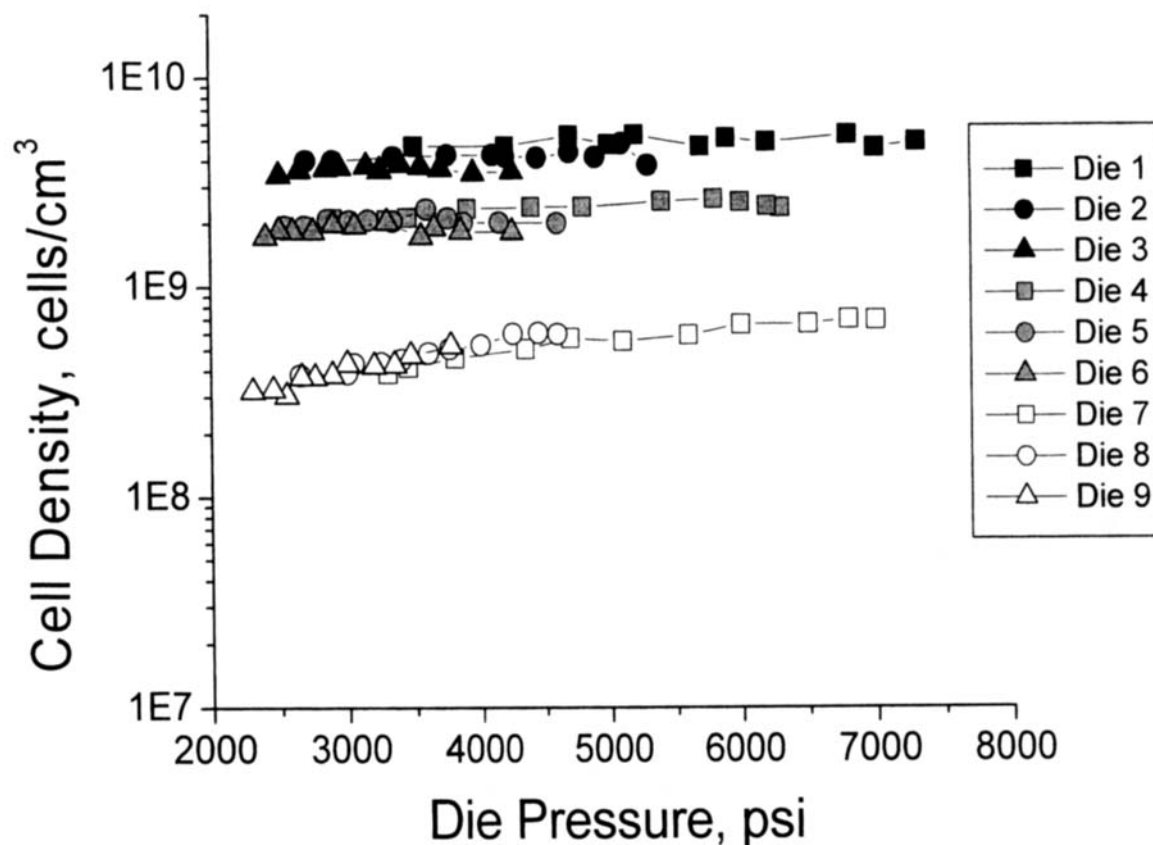
for detailed analysis. All the data points shown in Figs. 4–5 and 7–8 are the average of all the cell densities obtained at various die temperatures for each die or for each group. These experimental results revealed that the cell density was not significantly affected by the processing temperature.

Effect of the Die Geometry on Cell Nucleation Through Its Influence on Pressure-Drop Rate

Figure 4 shows the cell densities obtained at 1% talc content as a function of the pressure drop rate while varying the CO₂ content. Figure 5 shows the cell densities obtained at 2% CO₂ content while the talc content was varied. The results indicate that regardless of the amounts of nucleation agent and blowing agent, the cell density was significantly improved by applying a die with a high pressure-drop-rate geometry. This indicated that a large thermodynamic instability induced by a large pressure-drop rate is a critical factor affecting cell nucleation (11). Since the geometry of a die determines the pressure-drop rate when a polymer melt flows through the die, a properly designed die that generates a high pressure-drop rate is required to achieve a high cell density. Equation 5 shows that the smaller the nozzle diameter, the higher the pressure-drop rate for the same flow rate. However, there is a limit to the reduction of the nozzle diameter because of the manufacturability of the hole.

Furthermore, the diameter of a filamentary die may have to be determined most likely by the geometric requirements of the produced foams (although the determination of the die dimension for the required size of the produced foams is not an easy task because of the die swell and foam expansion). In this case, there is no room for varying the die geometry to enhance the cell density. Instead, the nucleating agent and blowing agent contents have to be increased to maximize the achievable cell density. On the other hand, the cell density can also be increased by increasing the flow rate (see Eq 5), which can be accomplished by increasing the speed of plasticating screw or the speed of gear pump. The increase of the flow rate may indicate that the extruder size should be upgraded.

Another way of increasing the cell density is to have a separate stage of cell nucleation before shaping in the die (41). In this case, the geometric dimension of the nucleation section can be independently determined to achieve the required pressure-drop rate while the geometric dimension of the shaping section can be independently determined to meet the size requirement of foam products. However, this approach may lead to a poor cell density of the final product because of cell coalescence that may occur as a result of the shear in the shaping section (42). If the pressure in the shaping section is low enough, the nucleated bubbles will quickly grow, and these grown cells may



interact with each other to cause coalescence of cells. Since this cell coalescence strongly depends on the relative size of the bubbles with respect to the distance of nuclei, the pressure in the shaping section will be the critical factor that governs the degree of cell coalescence. The pressure in the shaping section is determined by its resistance (i.e., the size of shaping section). Although lowering the temperature for the purpose of decreasing the gas diffusivity and increasing the melt strength would be helpful for decreasing the degree of cell coalescence, the size of the shaping section may not be increased much because the pressure in the shaping section may decrease much. If a large-sized extruder is used to cause a high flow rate, the pressure will increase, and therefore, the size of the shaping section may be increased without having a significant degree of cell coalescence. A further study is required to address the possibility of using a two-stage die for a thick cross-section product.

Effect of Shear Rate on Cell Nucleation

Although the majority of melt flowing in the core region in the filamentary die experiences a high pressure-drop rate due to the "plug flow" characteristics of shear-thinning, non-Newtonian melt (37), the melt flowing near the wall of die does not have a high pressure-drop rate because of the slow flow rate caused by

shear action from the die wall. However, most of the samples showed small variations in the cell density close to the surface because of the enhanced cell nucleation by the shear (30, 31). In fact, the cell densities close to the surface were observed to be slightly higher (up to 30%) than those of the core area in most cases as reported by Chen *et al.* (15, 17). The experimental results clearly indicate that the fast-flowing core region is nucleated by the high pressure-drop rate, whereas the slowly flowing surface region is nucleated by the shear action.

Effect of the Die Geometry on Cell Nucleation Through Its Influence on Die Pressure

The die pressure is a function of multiple variables, such as the speed of the plasticating screw (or the speed of gear pump), the kind and amount of blowing agent, the kind and amount of nucleating agent, the melt temperature (and its uniformity), the die temperature, and the die geometry. This complexity makes it difficult to study the effects of the die pressure on cell nucleation. In this context, the experimental study of the effects of the die pressure on the cell nucleation focused on two important aspects: the effects of die pressure change from varying the die temperature, and the effects of die pressure change from varying the die geometry.

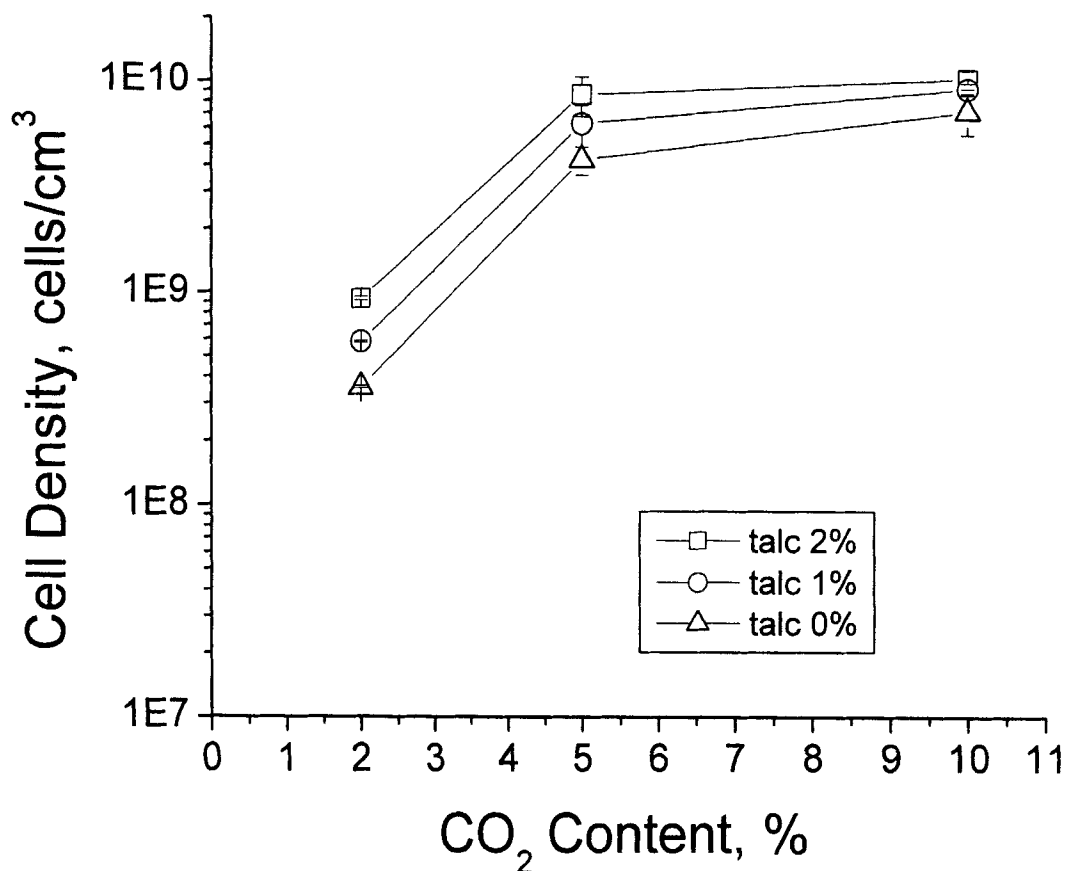
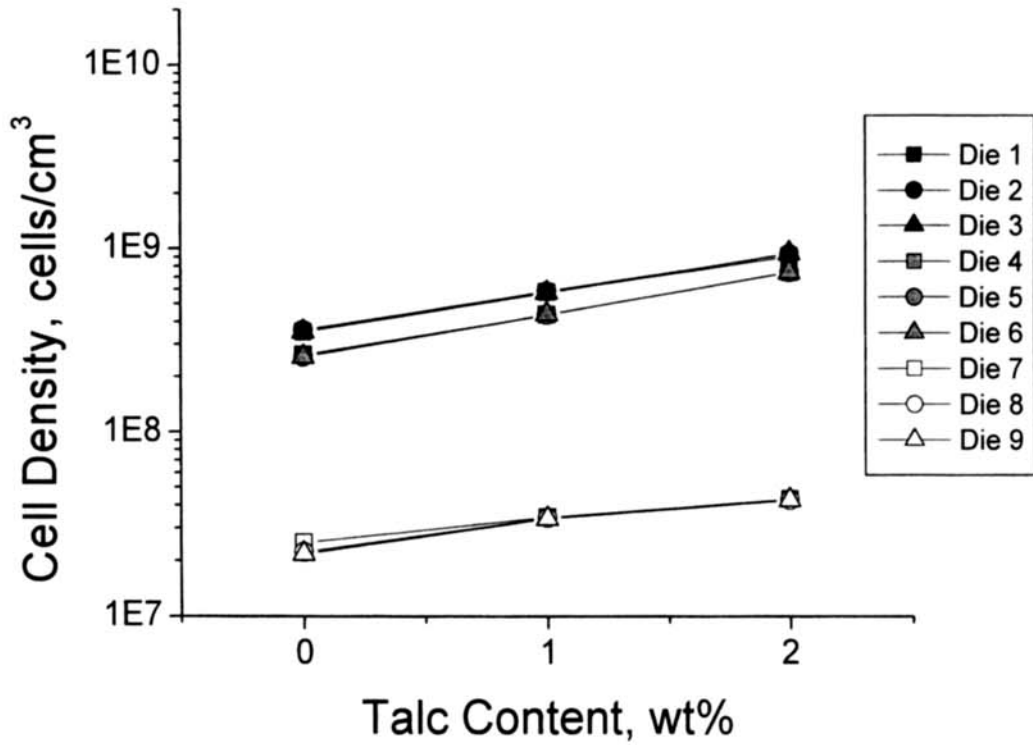


Fig. 7. Cell densities obtained at various CO₂ contents with Group 1 dies.

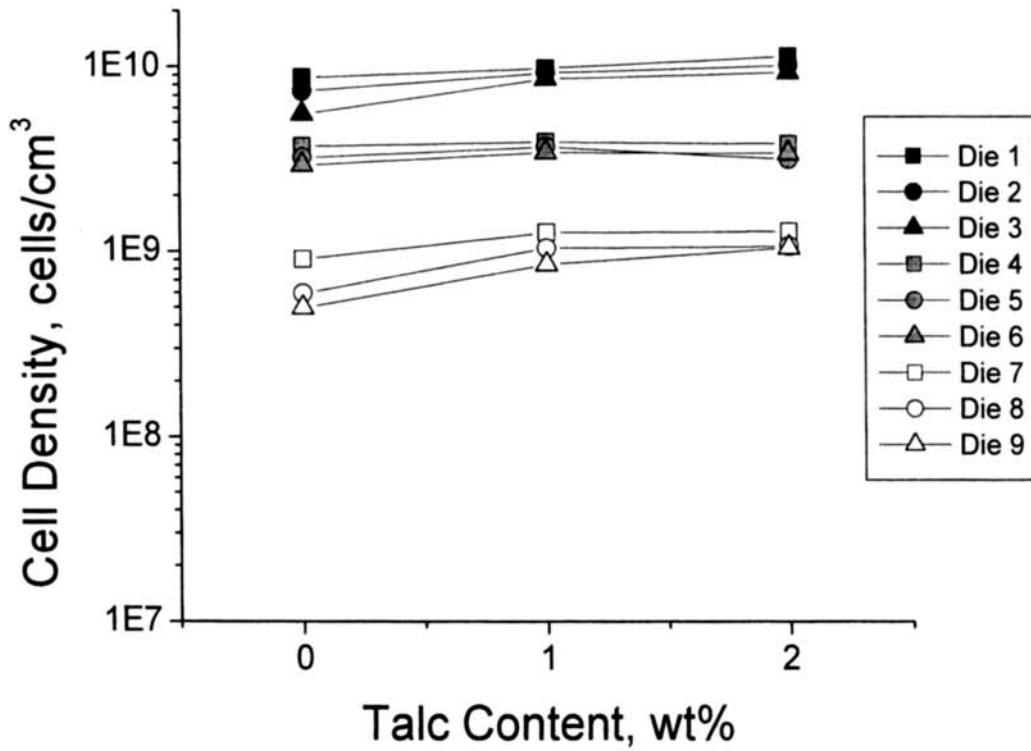
Overall, it appeared that the die pressure variations either by the die-temperature change or by the die-resistance change did not affect the cell density significantly. First of all, it was noted that as the temperature decreased, the die pressure increased because of the increased viscosity. However, the cell density of the foams produced from each die was observed to be almost constant irrespective of the die temperature as discussed before; i.e., it was mainly indifferent to the changes of the die pressure caused by the changes of the die temperature. Furthermore, the pressure change by varying the die geometry did not seem to affect the cell density, either. Figure 6 shows the cell density as a function of the die pressure for the 9 dies obtained with zero talc content and 5% CO₂ contents. Similar trends were observed for other talc and CO₂ contents. It turned out that each die group that has the same pressure-drop rate but a different die pressure showed almost the same cell density. In other words, when the die length was increased within the same die group, the pressure increased because of the increased resistance, but the experimentally observed cell density was not changed. Only the dies in Group 3 (Dies 7, 8, and 9) for the case of a high CO₂ content in the low pressure range, the cell density increased slightly as the die pressure increased. However, when

talc was added, all these dies in Group 3 showed exactly the same trends, and therefore, the pressure change due to the die-resistance change while fixing the diameter (i.e., within the same group) was not the main reason for this increase in the cell density. It is believed that this change was due to the characteristic of homogeneous cell nucleation, which is more sensitive to the pressure drop below the solubility pressure (11). On the other hand, the heterogeneously nucleated cell densities obtained with talc did not show any variations with respect to the die pressure. It is interesting to note that the cell densities did not decrease significantly as the pressure decreased even below the solubility pressure at each CO₂ content, which is estimated to be 6.2 MPa (900 psi), 15.2 MPa (2200 psi), and 30.3 MPa (4400 psi) for 2%, 5%, and 10% CO₂ contents at 200°C, respectively (33).

However, big bubbles were often observed in the extruded foams when the pressure was lower than the solubility pressure. This implied that below the solubility pressure, a portion of the gas was separated from the polymer matrix to create a second phase in a form of big gas pockets. But as the pressure was increased by lowering the temperature, those big gas pockets disappeared while the cell density was not significantly changed. The cell density would not be



(a)



(b)

Fig. 8. Cell densities obtained at various talc contents while varying the fixed CO₂ content: (a) 2% CO₂ (b) 10% CO₂.

affected much with the presence of these big pockets unless the cell nuclei closely located to the big bubbles are deteriorated significantly. Although the (nucleated) smaller cells in the vicinity of a big bubble tend to decrease their sizes because of cell coarsening (or cell ripening) (43), the deterioration of cell density due to cell coarsening is not expected to be severe in extrusion because the residence time of the nuclei in the die after cell nucleation is not very long (44). It should be noted that the cell density would be decreased proportionally to the volume fraction of big bubbles. But when the volume fraction of those big bubbles is not high, the cell-nuclei density would not be changed much with the non-dissolved gas pockets. This indicates again that the die pressure had almost no effect on the cell density, but greatly affected the cell morphology of the obtained foams, especially at low pressures.

Effect of CO₂ on Cell Nucleation

Figure 7 shows that for Group 1 dies, as the CO₂ content was increased, the cell density was increased accordingly, regardless of the talc content used in the experiments. Similar trends were also observed for other groups of dies. These results were expected because a greater degree of thermodynamic instability would be induced with a larger CO₂ content, and thereby, a larger cell density would be induced (10, 14). However, it was observed that the effect of CO₂ on the cell density was more pronounced when a die with a low pressure-drop-rate geometry was used at low talc contents. The cell density of PS foams blown with CO₂ did not seem to be increased significantly as the CO₂ content was increased from 5% to 10%.

Effect of Talc on Cell Nucleation

Figure 8 shows the effects of talc on the cell density obtained from the 9 dies. Although there was a trend of increasing the cell density at a high talc content, the results were not strikingly different. This means that for a PS-CO₂ system, the effect of talc is not dominant in the ranges of CO₂ contents and pressure-drop rates used in this study, although talc has proven to be an effective cell-nucleating agent for many combinations of plastic and blowing agent. It was observed that talc played a slightly stronger role at lower CO₂ concentrations in comparison with respective situations occurring at higher CO₂ concentrations. Although the sensitivity of cell density with respect to the talc content was not high, CO₂ and talc overall functioned complementarily in improving the cell nucleation for a given geometry of die.

SUMMARY AND CONCLUSIONS

This paper focuses on the effects of the die geometry on the nucleating behaviors of extruded PS foams resulting from its effects on the pressure-drop rate and the die pressure; meanwhile, the effects of CO₂ content and talc content through different dies were also investigated. The experimental study was conducted

using 3 groups of dies, 9 in total and 3 in each group, intended to have 3 different levels of pressures and pressure-drop rates.

The research presented in this paper confirmed that a proper die design plays a crucial role in improving the quality of extruded foams blown with CO₂. It was shown that regardless of the concentration of CO₂ or talc in the molten polymer, the die geometry determines the pressure-drop rate and the die pressure, thereby dominantly affecting both the cell density and the cell morphology. The pressure-drop rate was found to be the most significant factor to create a high cell density. When a high pressure-drop rate was created by applying a proper die geometry, a high microcellular cell density was achieved because a large thermodynamic instability was instigated. In contrast, the die pressure has insignificant effects on cell nucleation, although a high die pressure would be definitely favorable to completely dissolve the injected gas, and thereby to avoid the formation of big bubbles created by the undissolved gas pockets in the foam. It was observed that talc is a marginally favorable factor for nucleating cells in the PS-CO₂ system. Moreover, the CO₂ content, talc content, and die pressure-drop rate were observed to be complementary to each other in enhancing the cell density, but no synergistic effects were observed. When one of these parameters reached a very high value at low values of the other two, the cell density was solely governed by this parameter.

NOMENCLATURE

A = Dimensionless constant determined by the power-law characteristics of the polymer melt.

α = Area of a micrograph, m².

B = Dimensionless constant determined by the power-law characteristics of the polymer melt.

dp/dt = Pressure drop rate across the nozzle, Pa/s.

L = Length of the nozzle, m.

M = Dimensionless magnification factor of a micrograph.

m = Characteristic constant pertaining to a non-Newtonian fluid over a temperature range, N·s ^{n} /m².

N = Number of bubbles in a micrograph.

n = Dimensionless characteristic constant pertaining to a non-Newtonian fluid over a temperature range.

Q = Volume flow rate of the polymer/gas solution, m³/s.

R = Radius of the nozzle, m.

V_f = Void fraction of the extruded foam, %.

Δp = Pressure difference between a die's inlet and outlet, Pa.

Δt = Average residence time of the polymer/gas solution in the nozzle, s.

ρ_f = Density of the extruded foam, kg/m³.

ρ = Density of pure polymer, kg/m³.

REFERENCES

1. D. I. Collias, D. G. Baird, and R. J. M. Borggreve, *Polymer*, **25**, 18, 3978–3983 (1994).
2. D. I. Collias and D. G. Baird, *Polym. Eng. Sci.*, **35**, 1167 (1995).
3. K. A. Seeler and V. Kumar, *J. Reinf. Plas. Comp.*, **12**, 3, 359–376 (1993).
4. L. M. Matuana, C. B. Park, and J. J. Balatinez, *Cellular Polym.*, **17**, 1 (1998).
5. L. Glicksman, Notes from MIT Summer Program 4.10S Foams and Cellular Materials: Thermal and Mechanical Properties, Cambridge, MA, June 29–July 1 (1992).
6. L. M. Matuana, C. B. Park, and J. J. Balatinez, *Polym. Eng. Sci.*, **37**, 1137 (1997).
7. M. Shimbo, D. F. Baldwin, and N. P. Suh, *Polym. Eng. Sci.*, **35**, 1387 (1995).
8. M. Okada, A. Kabumoto, and M. Itoh, *Private Communication*, Furukawa Electric Co. (1997).
9. C. B. Park and N. P. Suh, *ASME Trans., J. Manuf. Sci. Eng.*, **118**, 4, 639–645 (1996).
10. C. B. Park and N. P. Suh, *Polym. Eng. Sci.*, **36**, 34 (1996).
11. C. B. Park, D. F. Baldwin, and N. P. Suh, *Polym. Eng. Sci.*, **35**, 432 (1995).
12. D. F. Baldwin, C. B. Park, S. W. Cha, and N. P. Suh, Canada Patent CA2107355 (1999).
13. C. B. Park and L. K. Cheung, *Polym. Eng. Sci.*, **37**, 1 (1997).
14. C. B. Park, L. K. Cheung, and S.-W. Song, *Cellular Polymers*, **17**, 4, 221–251 (1998).
15. H. Sheth, X. Wang, and L. Chen, *Foams*, 127–131 (2000).
16. D. Rodrigue, C. Woelfle, and L. E. Daigneault, *Blowing Agents and Foaming Process Conference*, Paper 22 (2001).
17. L. Chen, K. Blizard, and X. Wang, *SPE ANTEC Technical Papers*, **47**, 1726 (2001).
18. W. Michaeli and S. Habibi-Naini, *Blowing Agents and Foaming Process Conference*, Paper 9 (2001).
19. K. W. Koelling, D. Tomasko, L. J. Lee, and X. Han, *SPE ANTEC Tech. Papers*, **46**, 1857 (2000).
20. K. W. Koelling, D. L. Tomasko, L. J. Lee, and X. Han, *SPE ANTEC Tech. Papers*, **47**, 1741 (2001).
21. E. J. Beckman, *FoamPlas' 2000*, 83–94 (2000).
22. R. Gendron and L. Daigneault, *SPE Topical Conference*, 71–88, Montreal (2001).
23. N. P. Suh, *Private Communication*, MIT-Industry Polymer Processing Program (1980).
24. K. Jacobsen and D. Pierick, *SPE ANTEC Tech. Papers*, **46**, 1929 (2000).
25. D. Pierick and K. Jacobsen, *Plast. Eng.*, 46–51 (2001).
26. D. Pierick and R. Janisch, *Blowing Agents and Foaming Process Conference*, Paper 19 (2001).
27. M. Amon and C. D. Denson, *Polym. Eng. Sci.*, **26**, 255 (1986).
28. S. Lee, in *Foam Extrusion: Principles and Practice*, Chap. 4, 81–124. S. T. Lee, ed., Technomic Publishing Company, Lancaster, Pa. (2000).
29. J. S. Colton and N. P. Suh, *Polym. Eng. Sci.*, **27**, 485 (1987).
30. S. T. Lee, *Polym. Eng. Sci.*, **33**, 418 (1993).
31. S. T. Lee, *SPE ANTEC Technical Papers*, **40**, 1992 (1994).
32. N. S. Ramesh, in *Foam Extrusion Principles and Practice*, Chap. 5, 125–43. S. T. Lee, ed., Technomic Publishing Company, Lancaster, Pa. (2000).
33. Y. Sato, M. Yurugi, K. Fujiwara, S. Takishima, and H. Masuoka, *Fluid Phase Equilibria*, **125**, 129–138 (1996).
34. R. Straff, X. Wang, and L. Chen, *SPE ANTEC Technical Papers*, **47**, 1732 (2001).
35. A. de Waele, *Oil Color Chem. Assoc. J.*, **6**, 33 (1923).
36. W. Ostwald, *Kolloid-Z.*, **36**, 99 (1925).
37. R. B. Bird, R. C. Armstrong, and O. Hassager, *Dynamics of Polymeric Liquids, Fluid Mechanics, Vol. 1*, 233–51, Wiley (1977).
38. D. Klempner and K. C. Frisch, *Polymeric Foams*, Hanser (1991).
39. M. Lee, C. B. Park, and C. Tzoganakis, *Polym. Eng. Sci.*, **39**, 99 (1999).
40. J. M. Dealy and K. F. Wissburn, *Melt Rheology and Its Role in Plastics Processing*, Van Nostrand Reinhold (1990).
41. D. F. Baldwin, C. B. Park, and N. P. Suh, *Polym. Eng. Sci.*, **36**, 1425 (1996).
42. C. B. Park, A. H. Behraves, and R. D. Venter, in *Polymeric Foams: Science and Technology*, Chap. 8, 115–29, K. Khemani, ed., ACS, Washington, D.C. (1996).
43. G. Liu, C. B. Park, and J. A. Lefas, *Polym. Eng. Sci.*, **38**, 1997 (1998).
44. R. Pop-Iliev, PhD Thesis, University of Toronto (2002).